JACS
JOURNAL OF THE AMERICAN CHEMICAL SOCIETY
Communication
pubs.acs.org/JACS

Observation of α-Helical Hydrogen-Bond Cooperativity in an Intact Protein

Jingwen Li,[†,‡] Yefei Wang,[†,‡] Jingfei Chen,[†,‡] Zhijun Liu,[§] Ad Bax,[∥] and Lishan Yao*[,†,‡]

[†]Shandong Provincial Key Laboratory of Synthetic Biology and [‡]Laboratory of Biofuels, Qingdao Institute of Bioenergy and Bioprocess Technology, Chinese Academy of Sciences, Qingdao 266061, China

[§]National Center for Protein Science Shanghai, Institute of Biochemistry and Cell Biology, Shanghai Institutes for Biological Sciences, Chinese Academy of Sciences, Shanghai 201210, China

[∥]Laboratory of Chemical Physics, NIDDK, National Institutes of Health, Bethesda, Maryland 20892-0520, United States

Supporting Information

ABSTRACT: The presence and extent of hydrogen-bonding (H-bonding) cooperativity in proteins remains a fundamental question, which in the past has been studied extensively, mostly by infrared and fluorescence measurements on model peptides. We demonstrate that such cooperativity can be studied in an intact protein by hydrogen/deuterium exchange NMR spectroscopy. The method is based on the fact that substitution of NH by ND in a backbone amide group slightly weakens the N−H···O=C hydrogen bond. Our results show that such substitution at position i in an α-helix impacts the ^{1}H and ^{15}N chemical shifts of the amide sites of residues $i - 3$ to $i + 3$. Quantum mechanical calculations indicate that the upfield shifts of ^{1}H and ^{15}N resonances at site i, observed upon H/D exchanges at sites $i - 3$, $i + 1$, $i + 2$, and $i + 3$, correspond to a decrease of the ith backbone amide electric dipole moment, which weakens its H-bonding and long-range electrostatic interactions with other backbone amides in the α-helix. These results provide new quantitative insights into the cooperativity of H-bonding in protein α-helices.

Hydrogen bonds (H-bonds) provide directional interactions that play key roles in protein folding and structure stabilization. Computational studies indicate that H-bond cooperativity plays an important role in α-helix stabilization.[1−4] This cooperativity is stipulated to originate from the electric dipole moment of the α-helix, i.e, as the helix grows, the electric dipole moment of the newly added peptide plane forms favorable electrostatic interactions with the peptide planes of the existing helix, thereby increasing their dipole moments through polarization which then strengthens the electrostatic interaction among all peptide planes in the helix.[4] Whether or not analogous cooperativity applies to β-sheet formation is a function of the geometric details of any particular such structure and remains a matter of debate.[5−8] Cooperativity of α-helical H-bonding has been studied experimentally by multiple spectroscopic techniques, including time-resolved or 2D infrared spectroscopy[9−14] and T-jump fluorescence.[15−18] Only mass spectrometry has been proposed as a potential tool for studying cooperativity of H-bonding in intact proteins, relying on the exploitation of hydrogen/deuterium (H/D) exchange phenomena,[19,20] but to the best of our knowledge, no quantitative analysis of H-bond cooperativity of such data has yet been published. NMR spectroscopy is a particularly powerful tool for the study of H-bonding in biomolecules, which can be probed by chemical shifts,[21] NMR analysis of pressure-induced unfolding,[22] H-bond J couplings,[23−27] H/D fractionation factors,[28−32] and isotope shifts.[28,33,34]

Here, we demonstrate that even the cooperativity of H-bonding can be readily detected from H/D isotope shift effects observed for the ^{1}H and ^{15}N amide NMR signals of proximate peptide groups. Although such isotope shifts are very small, they can readily be separated, quantified, and assigned on the basis of experimentally determined pH-dependent amide solvent exchange rates. Such an analysis is demonstrated here for studying the H-bond cooperativity in the α-helix of GB3, a 56-residue model protein extensively studied by X-ray crystallography[35] and NMR.[36−38]

It is known that the change from ^{1}H to ^{2}H in a backbone amide N−H···O=C H-bond weakens the H-bond strength[39−41] through a lengthening of the donor−acceptor distance, commonly referred to as the classical Ubbelohde effect.[42] It is estimated that this weakening corresponds to a lengthening of the H−O distance by 0.02 ± 0.02 Å.[41] This increase is partially offset by a shortening of the N−D bond length, resulting from the anharmonicity of the N−H stretch vibration. The small changes of the H−O and N−H distances alter the electron distribution and thereby impact the chemical shifts of nuclei in nearby peptide planes, which forms the basis for our newly introduced NMR H/D exchange analysis method.

The H/D exchange experiments were carried out on the GB3 mutant E27Q, where the conservative E27Q mutation was introduced to simply eliminate an approximate overlap of the T25 and E27 amide signals in the ^{1}H−^{15}N HSQC spectrum of the native protein. When dissolving the protonated sample into a 15% H_2O/85% D_2O solvent at low temperatures (275 and 280 K) and low pH (4.3), only a few residues located near the two ends of the α-helix (A23−G38) showed detectable hydrogen exchange over a 12 h time period (Figure 1A, Supporting Information (SI), Table S1). Fitting of the intensities of each ^{1}H−^{15}N correlation in a time series ^{1}H−^{15}N HSQC spectra to an

Received: December 16, 2015
Published: February 8, 2016

DOI: 10.1021/jacs.5b13140
J. Am. Chem. Soc. 2016, 138, 1824−1827

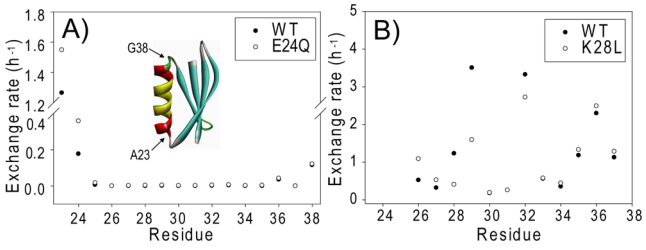

Figure 1. Effect of mutations on the backbone amide H/D exchange rates (k) of residues in the α helix (A23−G38) of GB3: (A) at low pH (4.3) and temperature (275 K); (B) at high pH (7.0) and temperature (298 K). The α helix is shown in the inset of panel A with residues E27−Y33 highlighted in yellow. In panel B, residues A23, E24, T25, and G38 have fast exchange rates (>∼6 h^{-1}) which cannot be determined from the measurements. The error of the exchange rate is ∼0.01 h^{-1} based on the goodness of the fitting.

exponential function was used to obtain the exchange rates k (Table S1). As the hydrogen exchange progresses, the ^{15}N (and ^{1}H) chemical shifts of other proximate amide groups show small changes (Figure 2), which result from the change in the H-bond

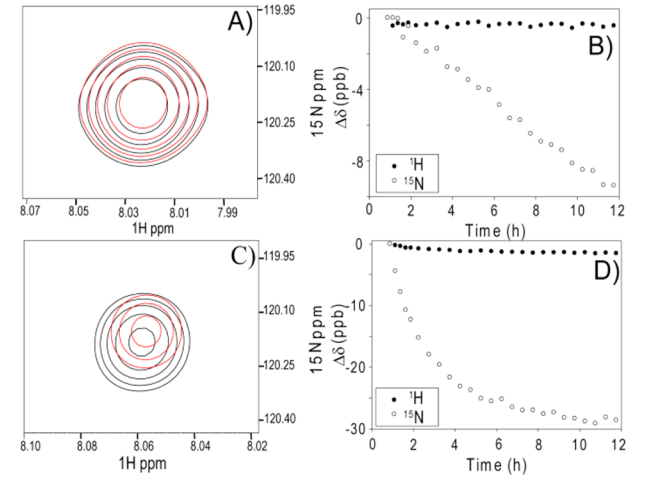

Figure 2. ^{1}H, ^{15}N chemical shift perturbation $\Delta\delta$ of residue Y33 in WT GB3, resulting from H/D exchange. (A, C) Overlay of the Y33 $^{1}H-^{15}N$ HSQC signals of the first (gray) and the last (red) spectrum of a recorded time series: (A) 275 K; (C) 298 K. The corresponding $\Delta\delta$ time profiles (B, 275 K; D, 298 K) are dominated by hydrogen exchange of (B) D36 and (D) A34 (fast component) and F30 and K31 (slow component).

strength of the exchanging amide group impacting the electron distribution around the observed backbone amide nuclei and thereby their chemical shifts. If only a single amide group in the protein were subject to hydrogen exchange over the 12 h time course that HSQC spectra were recorded, all observed chemical shift changes would be attributable to the H/D exchange of this one particular group. In practice, however, there are multiple nearby amide groups that all exchange with solvent, and it is therefore important to separately quantify the effects from all such nearby exchanging amide groups. For this purpose, the same measurements were also repeated at higher temperatures (298 and 303 K) and at pH of 7.0. Under these conditions, hydrogen exchange near the helix termini becomes much faster than the duration of a single HSQC measurement, and only the residues in the middle of the helix show H/D exchanges that are measurable over a 12 h time course (Figure 1B).

As can be seen in Figure 2, the changes in ^{1}H and ^{15}N chemical shifts resulting from the exchange of a nearby amide group are much smaller than the line width. In this limit, to a very good approximation, the measured peak position of amide i, $\delta_i(t)$, represents the average chemical shift, weighted according to the presence of H and D of the nearby exchanging amide group. After the protein is introduced to the 85% D_2O solvent, the backbone ^{15}N chemical shift change then can be fitted to the following eq (SI):

$$\Delta\delta_i(t) = \delta_i(t) - \delta_i(t_0) = 0.85 \sum_{j=1}^{n} \lambda_{ij}(\exp(-k_j t) - \exp(-k_j t_0)) \quad (1)$$

where $\delta_i(t)$ is the ^{15}N chemical shift at time t, λ_{ij} is the ^{15}N chemical shift change of site i due to the H/D exchange of amide site j, t_0 and t represent the midpoints of the first and subsequent HSQC measurements, and k_j is the H/D exchange rate of site j measured separately from the decaying intensity of the signal of amide j. With only four time series available for each backbone amide ^{15}N, ambiguity in assigning λ_{ij} to a specific exchanging amide, j, still remains. To solve this problem, the exchange experiments were also performed for a number of mutants (based on E27Q, hereafter referred to as wild-type, or "WT"), including V21A, V21L, E24Q, T25A, T25S, D36N, D36E, N37A, and N37Q for measurements at low pH (4.3) and temperatures (275 and 280 K) as well as K28L, A29S, K31L, and Q32N at higher pH (7.0) and temperature (298 and 303 K or 293 and 298 K). These mutations perturb the exchange rates, k, and thereby the observed $\Delta\delta$ values (Table S1).

To further remove ambiguity from the data analysis process, the number of fitted parameters was reduced by assuming that λ_{ij} is solely dependent on the separation, l, of helical residues i and j, i.e., on $l = j - i$. A global fit is then carried out for residues E27−Y33, in which λ_{ij} is assumed to be invariant as long as the difference $l = j - i$ is the same (so that λ_{ij} can be written as λ_l). The exchange rate k_j obtained from the exponential fit of the peak intensity (SI eq S2) is utilized in the $\Delta\delta$ fitting. The reduced $\chi^2 = \sum_{i=1}^{N}(\Delta\delta^i_{exp} - \Delta\delta^i_{pred})^2/N$ is then used to evaluate the goodness of the fit, where the summation extends over all N fitted chemical shifts, and $\Delta\delta_{exp}$ and $\Delta\delta_{pred}$ are the experimental and predicted (cf. eq 1) ^{15}N chemical shifts, respectively. An integer parameter m is introduced in the fitting with $|l| \leq m$, e.g., $m = 2$ corresponds to the model fitted using the sites $l = \pm 1, \pm 2$. As m increases, the χ^2 value decreases, and a large drop occurs when m changes from 2 to 3, suggesting that the $i - 3$ and/or $i + 3$ sites contribute significantly to $\Delta\delta$ (Figure 3A). The χ^2 value reaches a plateau when $m \geq 3$, indicating that the contributions from sites $i - 4$ and $i + 4$ are not significant. The F-test also supports that the improvement of the fitting is statistically significant up to $m = 3$ (Table S2). Thus, the final fitting results only include sites from $l = -3$ to $+3$ ($m = 3$), with the λ_l values listed in Table 1. All the sites have negative λ values except for site $i - 2$ which has a small positive value. The absolute values of λ from the sites with $l > 0$ are much larger than those with $l < 0$. That is to say, the subsequent sites contribute more than the preceding sites to $\Delta\delta$ of site i. In the fitting it is assumed that λ_{ij} only depends on l. With this assumption, the χ value for the $m = 3$ model is 2.2 ppb (Figure 3A), about 2-fold higher than the measurement error of 1 ppb. This result indicates that the variation of λ_{ij} is small and approaches the measurement error for pairs i and j with the same l. Extracting this variation, which reflects sequence dependence of the H-bond cooperativity and which our results show to be

DOI: 10.1021/jacs.5b13140
J. Am. Chem. Soc. 2016, 138, 1824−1827

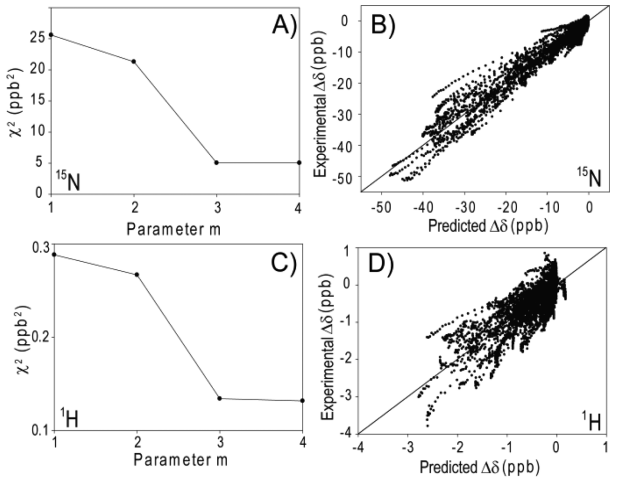

Figure 3. Fitting of the time series of $\Delta\delta$ values observed for residues E27−Y33, measured at four temperatures in WT GB3 and 13 mutants. (A) Reduced χ^2 as a function of the number m of nearest neighbors included in a global fit of the ^{15}N $\Delta\delta$ values of residues E27−Y33 to eq 1. As the number of neighboring sites increases, χ^2 decreases until reaching a plateau when $m \geq 3$. (B) Experimental versus predicted $\Delta\delta$ values for m = 3, yielding a Pearson correlation coefficient R_p of 0.98. As an example, the predicted and experimental $\Delta\delta$ time courses for residue A29 are shown in Figure S2. (C) Reduced χ^2 of the ^{1}H $\Delta\delta$ fitting to eq 1 for the same residues. (D) Correlation between the predicted and experimental ^{1}H $\Delta\delta$ values, yielding R_p = 0.82.

Table 1. λ Values (ppb) Globally Fitted for α-Helical Residues E27−Y33 in GB3

	λ_{-3}	λ_{-2}	λ_{-1}	λ_{+1}	λ_{+2}	λ_{+3}
^{15}N	−2.8±0.9[a]	4.0±2.9	−1.6±2.4	−21.5±2.3	−23.1±2.5	−29.4±1.9
^{1}H	−1.1±0.1	0.5±0.3	1.7±0.3	−1.2±0.3	−1.7±0.4	−2.0±0.3

[a]The error is based on a jackknife analysis of the data.

about an order of magnitude smaller than the average λ_l (for l = 1−3), is not possible at the accuracy available in our experimental data.

The $\Delta\delta$ values of the backbone amide ^{1}H were also fitted in the same way as for ^{15}N. However, the much smaller amplitude of the ^{1}H $\Delta\delta$ values (Figure 2B,D) results in a fitting accuracy that is considerably lower than for ^{15}N. Nevertheless, it is apparent that the main $\Delta\delta$ contributions also result from H/D exchange at sites $i-3$ to $i+3$, analogous to what was observed for ^{15}N.

To help interpret the experimentally measured isotope shifts, quantum mechanical (QM) calculations were performed for a H-bonded tri-*N*-methylacetamide ($(NMA)_3$) complex, built with a geometry that matches the peptide groups of the backbone peptide moieties of F30, Y33, and D36 in the structure of GB3 (PDB entry 2N7J).[38] Unlike in the experiment where the ^{1}H (or ^{15}N) chemical shift change $\Delta\delta$ of site i is composed of contributions from different sites, that each are subject to H/D exchange, in the calculations only the H-bond between sites i and $i-3$ (with the C═O group belonging to $i-4$) is perturbed by lengthening the H-bond distance d_{N-O} (Figure 4A) and then monitoring the chemical shift changes at sites $i+3$ and $i-3$, which correspond to λ_{-3} and λ_{+3}, respectively. Details of the QM calculations are described in the SI. The QM calculations predict that the λ values of both ^{15}N and ^{1}H are negative with the former about 20 times larger than the latter and that λ_{+3} is also considerably larger than λ_{-3}, especially for ^{15}N, consistent with

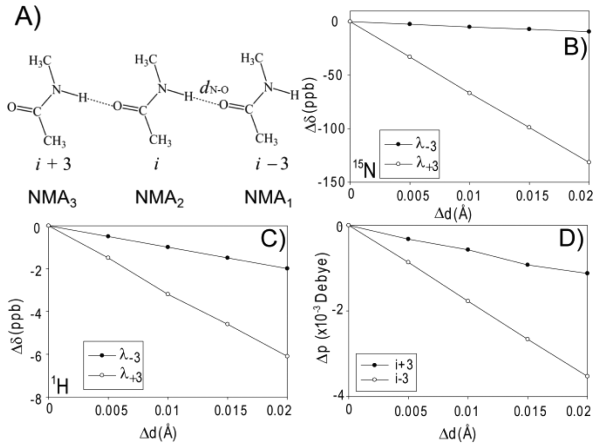

Figure 4. QM calculations of the H-bonding effect on chemical shifts and dipole moments in a model tri-NMA complex (A). The peptide plane atomic coordinates and H-bond geometry of the complex are taken from the peptide groups involving the amides of F30, Y33, and D36 in the GB3 structure. The H-bond distance d_{N-O} was increased from 2.929 Å in steps of 0.005 Å, with all other degrees of freedom frozen. The calculated λ values of (B) ^{15}N and (C) ^{1}H of NMA_1 (λ_{+3}) and NMA_3 (λ_{-3}) decrease as the distance increases. (D) The accompanying decrease in dipole moments of NMA_1 and NMA_3 indicates a weakening of the polarization of these two peptide planes.

the experimental findings (Figure 4B,C, Table 1). Values comparable with the experimental $\lambda_{\pm3}$ are obtained for a d_{N-O} elongation of 0.005 Å, with the corresponding λ_{+3} (λ_{-3}) of −1.6 (−0.6) ppb for ^{1}H and −34 (−2.4) ppb for ^{15}N (Figure 4A). The elongation of d_{N-O} also decreases the electric dipole moments of NMA_1 and NMA_3, and the amplitude of the decrease for NMA_1 is about three times larger than for NMA_3 (Figure 4D). The QM calculations indicate that the decrease of the ^{15}N and ^{1}H chemical shifts, caused by the redistribution of the electron density, corresponds to a decrease of the peptide plane electric dipole moment. The negative values of λ_{-3}, λ_{+1}, λ_{+2}, and λ_{+3} for both ^{1}H and ^{15}N (Table 1) then imply that the substitution of H by D at all of these four sites decreases the dipole moment of the ith peptide plane (depolarization), which thereby weakens its H-bonding and electrostatic interactions with other peptide planes. This result is a clear illustration of the H-bond cooperativity in the α-helix. Meanwhile, a weak but surprising anticooperativity is observed for the site $i-2$, whereas for the site $i-1$ the cooperativity is nearly zero, and λ_{-1} has opposite signs for ^{1}H and ^{15}N. From a geometric point of view, the amide groups of sites $i-1$, $i-2$, and $i-3$ ($l>0$) are proximate to both the donor and acceptor atoms of the $i \rightarrow i-3$ H-bond where the exchange occurs, whereas the sites $i+1$, $i+2$, and $i+3$ ($l<0$) are only close to the H-bond donor. This implies that $|\lambda_l|$ ($l>0$) should be larger than $|\lambda_l|$ ($l<0$), as obtained from the experimental measurement. More sophisticated QM calculations may provide better insights.[43,44] As mentioned above, the effect of conservative mutations on $\Delta\delta$ approaches the measurement error. However, the effect of nonconservative mutations, or structure-inducing osmolytes such as trimethylamine oxide (TMAO), is likely to be considerably larger and may become accessible through a study of the type described here.

It is desirable to convert the λ values to cooperativity in energetic terms. A λ value of 25 ppb corresponds to a decrease of the dipole moment by 0.7×10^{-3} Debye (Figure 4D). The dipole moment of NMA is 5.8 D, and the H-bond energy is ∼8 kcal/mol (SI). The 0.012% decrease of the dipole moment therefore

DOI: 10.1021/jacs.5b13140
J. Am. Chem. Soc. 2016, 138, 1824−1827

corresponds to a H-bond energy loss of 1 cal/mol. Large ^{15}N λ_l values for l = 1−3 suggest that these three peptide planes are affected the most. Since each peptide plane forms two H-bonds and the H-bond between i and $i-3$ needs to be excluded, a total of five H-bonds are weakened in response to the H/D exchange at a specific site i, yielding a total energy loss of ∼5 cal/mol. It previously was estimated that H/D exchange decreases the $i \rightarrow i-3$ H-bond energy by 20 cal/mol, based on the weakening of the $^{3h}J_{NC}$ coupling.[41] Combining these two numbers yields a cooperativity of ∼25%, in line with the cooperativity value of 33% for a polyalanine α-helix from DFT calculations.[45]

In summary, we have shown that H-bonding cooperativity in the α-helix of protein GB3 can readily be studied by the newly introduced H/D exchange NMR method. We have shown that H/D exchange at backbone amide sites $i-3$ to $i+3$ all perturb the backbone ^{15}N and ^{1}H chemical shifts at amide site i. Although minute, these chemical shift changes are readily measured at high precision and provide novel experimental data on H-bond cooperativity in an α-helix. The same technology can be used to study H-bond cooperativity in β-sheets, and we are currently pursuing such studies. Analogously, the method can also be used to investigate H-bond cooperativity in other biomolecules such as DNA and RNA.

■ ASSOCIATED CONTENT

Supporting Information

The Supporting Information is available free of charge on the ACS Publications website at DOI: 10.1021/jacs.5b13140.

Experimental procedures and additional data (PDF)

■ AUTHOR INFORMATION

Corresponding Author

*yaols@qibebt.ac.cn

Notes

The authors declare no competing financial interest.

■ ACKNOWLEDGMENTS

This work was supported by the National Natural Science Foundation of China (Grant no. 21173247 and 31270785 to L.Y.). A.B. is supported by the Intramural Research Program of the NIDDK, National Institutes of Health (NIH).

■ REFERENCES

(1) Wieczorek, R.; Dannenberg, J. J. *J. Am. Chem. Soc.* **2003**, *125*, 8124.
(2) Wieczorek, R.; Dannenberg, J. J. *J. Am. Chem. Soc.* **2003**, *125*, 14065.
(3) Kobko, N.; Paraskevas, L.; del Rio, E.; Dannenberg, J. J. *J. Am. Chem. Soc.* **2001**, *123*, 4348.
(4) Morozov, A. V.; Tsemekhman, K.; Baker, D. *J. Phys. Chem. B* **2006**, *110*, 4503.
(5) Viswanathan, R.; Asensio, A.; Dannenberg, J. J. *J. Phys. Chem. A* **2004**, *108*, 9205.
(6) Rossmeisl, J.; Norskov, J. K.; Jacobsen, K. W. *J. Am. Chem. Soc.* **2004**, *126*, 13140.
(7) Zhao, Y. L.; Wu, Y. D. *J. Am. Chem. Soc.* **2002**, *124*, 1570.
(8) Woys, A. M.; Almeida, A. M.; Wang, L.; Chiu, C. C.; McGovern, M.; de Pablo, J. J.; Skinner, J. L.; Gellman, S. H.; Zanni, M. T. *J. Am. Chem. Soc.* **2012**, *134*, 19118.
(9) Williams, S.; Causgrove, T. P.; Gilmanshin, R.; Fang, K. S.; Callender, R. H.; Woodruff, W. H.; Dyer, R. B. *Biochemistry* **1996**, *35*, 691.
(10) Lakhani, A.; Roy, A.; De Poli, M.; Nakaema, M.; Formaggio, F.; Toniolo, C.; Keiderling, T. A. *J. Phys. Chem. B* **2011**, *115*, 6252.
(11) Tucker, M. J.; Abdo, M.; Courter, J. R.; Chen, J. X.; Brown, S. P.; Smith, A. B.; Hochstrasser, R. M. *Proc. Natl. Acad. Sci. U. S. A.* **2013**, *110*, 17314.
(12) Zeko, T.; Hannigan, S. F.; Jacisin, T.; Guberman-Pfeffer, M. J.; Falcone, E. R.; Guildford, M. J.; Szabo, C.; Cole, K. E.; Placido, J.; Daly, E.; Kubasik, M. A. *J. Phys. Chem. B* **2014**, *118*, 58.
(13) Lin, M. M.; Shorokhov, D.; Zewail, A. H. *Proc. Natl. Acad. Sci. U. S. A.* **2014**, *111*, 14424.
(14) Lai, J. K.; Kubelka, G. S.; Kubelka, J. *Proc. Natl. Acad. Sci. U. S. A.* **2015**, *112*, 9890.
(15) Thompson, P. A.; Eaton, W. A.; Hofrichter, J. *Biochemistry* **1997**, *36*, 9200.
(16) Ihalainen, J. A.; Paoli, B.; Muff, S.; Backus, E. H. G.; Bredenbeck, J.; Woolley, G. A.; Caflisch, A.; Hamm, P. *Proc. Natl. Acad. Sci. U. S. A.* **2008**, *105*, 9588.
(17) Lin, M. M.; Mohammed, O. F.; Jas, G. S.; Zewail, A. H. *Proc. Natl. Acad. Sci. U. S. A.* **2011**, *108*, 16622.
(18) Davis, C. M.; Cooper, A. K.; Dyer, R. B. *Biochemistry* **2015**, *54*, 1758.
(19) Miranker, A.; Robinson, C. V.; Radford, S. E.; Dobson, C. M. *Faseb J.* **1996**, *10*, 93.
(20) Krantz, B. A.; Srivastava, A. K.; Nauli, S.; Baker, D.; Sauer, R. T.; Sosnick, T. R. *Nat. Struct. Biol.* **2002**, *9*, 458.
(21) Wagner, G.; Pardi, A.; Wuthrich, K. *J. Am. Chem. Soc.* **1983**, *105*, 5948.
(22) Dellarole, M.; Caro, J. A.; Roche, J.; Fossat, M.; Barthe, P.; Garcia-Moreno, B.; Royer, C. A.; Roumestand, C. *J. Am. Chem. Soc.* **2015**, *137*, 9354.
(23) Cordier, F.; Grzesiek, S. *J. Am. Chem. Soc.* **1999**, *121*, 1601.
(24) Cornilescu, G.; Ramirez, B. E.; Frank, M. K.; Clore, G. M.; Gronenborn, A. M.; Bax, A. *J. Am. Chem. Soc.* **1999**, *121*, 6275.
(25) Grzesiek, S.; Cordier, F.; Jaravine, V.; Barfield, M. *Prog. Nucl. Magn. Reson. Spectrosc.* **2004**, *45*, 275.
(26) Sass, H.-J.; Schmid, F. F.-F.; Grzesiek, S. *J. Am. Chem. Soc.* **2007**, *129*, 5898.
(27) Nisius, L.; Grzesiek, S. *Nat. Chem.* **2012**, *4*, 711.
(28) Vakonakis, I.; Salazar, M.; Kang, M. J.; Dunbar, K. R.; LiWang, A. C. *J. Biomol. NMR* **2003**, *25*, 105.
(29) Loh, S. N.; Markley, J. L. *Biochemistry* **1994**, *33*, 1029.
(30) LiWang, A. C.; Bax, A. *J. Am. Chem. Soc.* **1996**, *118*, 12864.
(31) Coman, D.; Russu, I. M. *J. Am. Chem. Soc.* **2003**, *125*, 6626.
(32) Li, G. C.; Srivastava, A. K.; Kim, J.; Taylor, S. S.; Veglia, G. *Biochemistry* **2015**, *54*, 4042.
(33) Vakonakis, I.; LiWang, A. C. *J. Am. Chem. Soc.* **2004**, *126*, 7152.
(34) Manalo, M. N.; Perez, L. M.; LiWang, A. *J. Am. Chem. Soc.* **2007**, *129*, 11298.
(35) Derrick, J. P.; Wigley, D. B. *J. Mol. Biol.* **1994**, *243*, 906.
(36) Markwick, P. R. L.; Bouvignies, G.; Blackledge, M. *J. Am. Chem. Soc.* **2007**, *129*, 4724.
(37) Granata, D.; Camilloni, C.; Vendruscolo, M.; Laio, A. *Proc. Natl. Acad. Sci. U. S. A.* **2013**, *110*, 6817.
(38) Li, F.; Grishaev, A.; Ying, J.; Bax, A. *J. Am. Chem. Soc.* **2015**, *137*, 14798.
(39) Engler, N.; Ostermann, A.; Niimura, N.; Parak, F. G. *Proc. Natl. Acad. Sci. U. S. A.* **2003**, *100*, 10243.
(40) Kachalova, G. S.; Popov, A. N.; Bartunik, H. D. *Science* **1999**, *284*, 473.
(41) Jaravine, V. A.; Cordier, F.; Grzesiek, S. *J. Biomol. NMR* **2004**, *29*, 309.
(42) Ubbelohde, A. R.; Gallagher, K. J. *Acta Crystallogr.* **1955**, *8*, 71.
(43) Kita, Y.; Kamikubo, H.; Kataoka, M.; Tachikawa, M. *Chem. Phys.* **2013**, *419*, 50.
(44) Kanematsu, Y.; Tachikawa, M. *J. Chem. Phys.* **2014**, *141*, 185101.
(45) Hua, S.; Xu, L.; Li, W.; Li, S. *J. Phys. Chem. B* **2011**, *115*, 11462.

DOI: 10.1021/jacs.5b13140
J. Am. Chem. Soc. 2016, 138, 1824−1827